Mass Spectrometry Based Approach to Study the Kinetics of O-6-Alkylguanine DNA Alkyltransferase-Mediated Repair of O-6-Pyridyloxobutyl-2 '-deoxyguanosine Adducts in DNA

ARTICLE *in* CHEMICAL RESEARCH IN TOXICOLOGY · SEPTEMBER 2011

Impact Factor: 3.53 · DOI: 10.1021/tx2002993 · Source: PubMed

Published in final edited form as:
Chem Res Toxicol. 2011 November 21; 24(11): 1966–1975. doi:10.1021/tx2002993.

Mass Spectrometry Based Approach to Study the Kinetics of O^6-Alkylguanine DNA Alkyltransferase Mediated Repair of O^6-pyridyloxobutyl-2′-deoxyguanosine Adducts in DNA

Delshanee Kotandeniya[†], **Dan Murphy**[†], **Uthpala Seneviratne**[†], **Rebecca Guza**, **Anthony Pegg**[€], **Sreenivas Kanugula**[€], and **Natalia Tretyakova**[†,*]

[†]Department of Medicinal Chemistry and the Masonic Cancer Center, University of Minnesota, Minneapolis, Minnesota 55455

[€]Department of Cellular and Molecular Physiology, Pennsylvania State University College of Medicine, Hershey, Pennsylvania 17033

Abstract

O^6-POB-dG (O^6-[4-oxo-4-(3-pyridyl)but-1-yl]deoxyguanosine) are promutagenic nucleobase adducts that arise from DNA alkylation by metabolically activated tobacco-specific nitrosamines such as 4-(methylnitrosamino)- 1-(3-pyridyl)-1-butanone (NNK) and N-nitrosonicotine (NNN). If not repaired, O^6-POB-dG adducts cause mispairing during DNA replication, leading to G → A and G → T mutations. A specialized DNA repair protein, O^6-alkylguanine-DNA-alkyltransferase (AGT), transfers the POB group from O^6-POB-dG in DNA to a cysteine residue within the protein (Cys145), thus restoring normal guanine and preventing mutagenesis. The rates of AGT-mediated repair of O^6-POB-dG may be affected by local DNA sequence context, potentially leading to adduct accumulation and increased mutagenesis at specific sites within the genome. In the present work, isotope dilution high performance liquid chromatography-electrospray ionization tandem mass spectrometry (HPLC-ESI$^+$-MS/MS)-based methodology was developed to investigate the influence of DNA sequence on the kinetics of AGT-mediated repair of O^6-POB-dG adducts. In our approach, synthetic DNA duplexes containing O^6-POB-dG at a specified site are incubated with recombinant human AGT protein for defined periods of time. Following spiking with D_4-O^6-POB-dG internal standard and mild acid hydrolysis to release O^6-POB-guanine (O^6-POB-G) and D_4-O^6-POB-guanine (D_4-O^6-POB-G), samples are purified by solid phase extraction (SPE), and O^6-POB-G adducts remaining in DNA are quantified by capillary HPLC-ESI$^+$-MS/MS. The new method was validated by analyzing mixtures containing known amounts of O^6-POB-dG-containig DNA and the corresponding unmodified DNA duplexes and by examining the kinetics of alkyl transfer in the presence of increasing amounts of AGT protein. The disappearance of O^6-POB-dG from DNA was accompanied by pyridyloxobutylation of AGT Cys-145 as determined by HPLC-ESI$^+$-MS/MS of tryptic peptides. The applicability of the new approach was shown by determining the second order kinetics of AGT-mediated repair of O^6-POB-dG adducts placed within a DNA duplex representing modified rat *H-ras* sequence (5′-AATAGTATCT[O^6-POB-G]GAGCC-3′) opposite either C or T. Faster rates of alkyl transfer were observed when O^6-POB-dG was paired with T rather than C ($k = 1.74 \times 10^6\ M^{-1}s^{-1}$ *vs* $1.17 \times 10^6\ M^{-1}s^{-1}$).

[*]To whom correspondence should be addressed: Masonic Cancer Center, University of Minnesota, Mayo Mail Code 806, 420 Delaware St SE, Minneapolis, MN 55455, USA. phone: 612-626-3432 fax: 612-626-5135 trety001@umn.edu .

Introduction

4-(Methylnitrosamino)-1-(3-pyridyl)-1-butanone (NNK)* and N-nitrosonicotine (NNN) are carcinogenic nitrosamines found only in tobacco products and known to specifically induce lung cancer in laboratory animals.[1-3] The carcinogenic effects of NNK and NNN are mediated by the formation of promutagenic DNA adducts. Both tobacco-specific nitrosamines undergo cytochrome P450 monooxygenase-mediated bioactivation to form pyridyloxobutyl diazonium ions which react with nucleophilic sites in DNA. The resulting bulky pyridyloxobutylated nucleobase lesions include N7-[4-oxo-4-(3-pyridyl)-but-1-yl]deoxyguanosine (N7-POB-dG), O^6-[4-oxo-4-(3-pyridyl)but-1-yl]deoxyguanosine (O^6-POB-dG), O^2-[4-(3-pyridyl)-4-oxobut-1-yl]thymidine (O^2-POB-T), and O^2-[4-(3-pyridyl)-4-oxobut-1-yl]-deoxycytidine (O^2-POB-dC).[3,4] Among these, O^6-POB-dG have been shown to be strongly mutagenic. During replication, DNA polymerases incorporate either thymine or adenine opposite O^6-POB-dG in lieu of the correct base (cytosine), leading to G → A transitions and G → T transversions.[5]

In order to prevent mutagenesis, O^6-POB-dG lesions must be efficiently repaired prior to DNA replication. A specialized DNA repair protein, O^6-alkylguanine-DNA alkyltransferase (AGT), directly removes the O^6 -alkyl group from modified guanine such as O^6-POB-G, restoring the native DNA structure.[6-8] Upon AGT binding to double-stranded DNA, the O^6-alkylguanosine residue is flipped out of the DNA base stack to enter the active site of the AGT protein.[9] Histidine-146 residue in the AGT active site, with the aid of a water molecule, acts as a general base to abstract a proton from the thiol group of a neighboring cysteine-145 (Cys145).[6,9] The resulting thiolate anion accepts the alkyl group from O^6-alkylguanosine, restoring normal guanine and forming a thioether at Cys145 (Scheme 1). This inactivates the AGT protein by inducing conformational changes, ubiquitination, and proteosomal degradation.[10,11] As a result, the AGT repair reaction is stoichiometric, inactivating one molecule of AGT protein per each alkylguanine lesion repaired.

All available evidence suggests that alkylated AGT molecules are not re-activated but are rapidly degraded by the proteasome. Several hypotheses have been put forward to explain this unusual mechanism,[8,12] which may relate to the difficulty of distinguishing O^6-methylguanine from unmodified guanine at a high enough level of discrimination to prevent damage to normal DNA.[8] Furthermore, although one molecule of protein is used up per adduct repaired, only a single protein is needed as compared to over 20 proteins in the nucleotide excision repair mechanism. Finally, the alkylated protein must be degraded quickly because it retains its DNA-binding abilities and may interfere with repair of additional O^6-alkylguanine lesions.

While several studies have reported that the rates of AGT-mediated repair of O^6-POB-dG lesions are affected by neighboring DNA bases, only a few selected DNA sequences have been examined.[13,14] Coulter et. al. used a radioflow HPLC-based methodology to show that the first order rate for AGT-mediated repair of O^6-POB-dG placed in the first position of the *H-ras* codon 12 (5′-CT**X**GA-3′ context, 0.95×10^{-4} s^{-1}) was ~ 6 times larger for the adduct placed at the second position of codon 12 (5′TG**X**AG-3′ context, 0.16×10^{-4} s^{-1}).[14] A

*Abbreviations AGT, O^6-alkylguanine-DNA-alkyltransferase; BSA, bovine serum albumin; O^6-Bz-dG, O^6-benzyl-deoxyguanosine; CID, collision induced dissociation; DTT, dithiothreitol; DNase I, deoxyribonuclease I; ESI-MS/MS, electrospray ionization tandem mass spectrometry; EDTA, ethylenediamine tetraacetic acid; HPLC-ESI-MS/MS, high performance liquid chromatography-electrospray ionization-tandem mass spectrometry; MALDI-TOF, matrix-assisted laser desorption-ionization with time of flight detection; N7-MeG, N7-methylguanine; O^6-Me-dG, O^6-methyl-2′-deoxyguanosine; O^6-Me-G, O^6-methylguanine; N7-POB-G, N7-[4-oxo-4-(3-pyridyl)-but-1-yl]guanine; NNK, 4-(methylnitrosamino)-1-(3-pyridyl)-1-butanone; O^6-POB-dG, O^6-[4-oxo-4-(3-pyridyl)but-1-yl]deoxyguanosine; D_4-O^6-POB-dG, D_4-O^6-[4-oxo-4-(3-pyridyl)but-1-yl]deoxyguanosine; O^6-POB-G, O^6-[4-oxo-4-(3-pyridyl)but-1-yl]guanine; PDE I, phosphodiesterase I; PDE II, phosphodiesterase II; POB, pyridyloxobutyl; SPE, solid phase extraction; SRM, selected reaction monitoring; TSQ, triple stage quadrupole.

much faster repair rate (0.022 s^{-1}) was observed for another sequence containing O^6-POB-dG (X) in 5′-AT**X**GC-4′ sequence context.[14] Similar results were reported by Mijal et. al.[13] who employed denaturing PAGE to examine the kinetics of AGT-mediated repair of O^6-POB-dG adducts relative to O^6-Me-dG within rat *H-ras* codon 12. These authors[13] also noted that the rate of O^6-POB-dG repair increased when a thymine rather than cytosine was placed in the complementary strand opposite O^6-alkyl-dG. However, to our knowledge, no systematic studies have been conducted to examine the effects of local DNA sequence on AGT-mediated repair of O^6-POB-dG, probably due to practical limitations of the available experimental methodologies. Previous studies have relied on the ability of HPLC or gel electrophoresis methodologies to resolve alkylated and dealkylated DNA strands.[13,14] Such separations can be quite challenging, especially for longer DNA duplexes (> 20 nucleotides).

In the present work, a novel, stable isotope dilution capillary HPLC electrospray ionization tandem mass spectrometry (ESI^+-MS/MS) methodology was developed to analyze the kinetics of AGT repair of O^6-POB-dG adducts *in vitro* as a function of DNA sequence context. An application of this new methodology was demonstrated for O^6-POB-dG lesions introduced into synthetic oligonucleotide duplexes representing *p53* codon 158 and a modified rat *H-ras* gene sequence containing codon 12.

Experimental Procedures

Materials

Dithiane protected O^6-POB-dG (O^6-[3-[2-(3-pyridyl)-1,3-dithyan-2-yl]propyl]-deoxyguanosine) was synthesized according to methods published by Wang and coworkers[15] and converted to 5′-dimethoxytrityl-*N*,*N*-dimethyl-formamidine-O^6-[4-oxo-4-(3-pyridyl)but-1-yl]-2′-deoxyguanosine, 3′-[(2-cyanoethyl)-(*N*,*N*-diisopropyl)]-phosphoramidite by standard phosphoramidite chemistry.[15,16] All other nucleoside phosphoramidites, solvents, and solid supports required for the solid phase synthesis of DNA were procured from Glen Research Corporation (Sterling, VA). Human recombinant AGT protein with a C-terminal histidine tail (WT ch-AGT) was expressed in *E. coli* and isolated as reported previously.[17,18] The catalytic activity of the AGT protein was determined by incubating with known amounts of DNA duplexes containing O^6-MeG.[19] Approximately 75% of the total protein was active, depending on the aliquot. D_4-O^6-POB-dG was a gift from Professor Stephen Hecht (University of Minnesota). O^6-POB-dG-containing oligodeoxynucleotide representing a modified rat *H-ras* gene sequence was generously provided by Professor Lisa Peterson (University of Minnesota). Phosphodiesterase I, phosphodiesterase II, and DNase I were obtained from Worthington Biochemical Corporation (Lakewood, NJ). Trypsin was purchased from Promega (Madison, WI), and bovine intestinal alkaline phosphatase was procured from Sigma Aldrich Chemical Company (Milwaukee, WI). The rest of the chemicals were purchased either from Fisher Scientific (Fairlawn, NJ) or Sigma-Aldrich (Milwaukee, WI).

Solid Phase Synthesis of DNA

Synthetic oligodeoxynucleotides containing O^6-[3-[2-(3-pyridyl)-1,3-dithian-2-yl]propyl]-deoxyguanosine in the context of *p53* codon 158 were prepared by solid phase synthesis on a DNA synthesizer[16] starting with synthetic 5′-dimethoxytrityl-*N*,*N*-dimethyl-formamidine-O^6-[4-oxo-4-(3-pyridyl)but-1-yl]-2′-deoxyguanosine, 3′-[(2-cyanoethyl)-(*N*,*N*-diisopropyl)]-phosphoramidite.[15] Following HPLC purification of synthetic oligonucleotides, the 1,3-dithiane protective group was removed with *N*-chlorosuccinimide to produce the corresponding O^6-POB-G-containing DNA.[15,20]

Synthetic DNA oligomers were purified by reversed phase HPLC using an Agilent 1100 HPLC system interfaced with a DAD UV detector.[21,22] HPLC fractions corresponding to oligodeoxynucleotides of interest were collected and concentrated under reduced pressure. The presence of O^6-POB-dG was confirmed by capillary HPLC-ESI$^-$ MS (Table 1).[22-24] Oligonucleotide concentrations were determined from the amounts of 2′-deoxyguanosine present in enzymatic digests using a previously published protocol.[19,25,26]

O^6-POB-dG containing DNA duplexes were prepared by mixing equal amounts of the complimentary strands in 10 mM Tris-HCl (pH 8) buffer containing 50 mM NaCl to achieve a final concentration of 200 μM, followed by heating at 90 °C for 5 minutes and slow cooling to room temperature.[25]

AGT reactions with O^6-POB-dG containing DNA Duplexes

DNA duplexes containing O^6-POB-dG (500 fmol, Table 1) were mixed with human recombinant AGT protein (400 fmol) in a final volume of 90 μl of 50 mM Tris-HCl buffer (pH 7.8) containing 0.1 mM EDTA, 0.5 mg/mL BSA, and 0.5 mM DTT. Following incubation at room temperature for fixed periods of time (0-50 seconds), repair reactions were manually quenched with 0.2 N HCl. D_4-O^6-POB-dG internal standard (250 fmol) was added, and the DNA was subjected to mild acid hydrolysis (0.1 N HCl, 70 °C for 1 h). Samples were neutralized with ammonium hydroxide. O^6-POB-G adducts were isolated by solid phase extraction (SPE) and quantified by the capillary HPLC-ESI$^+$-MS/MS as described below.

Solid Phase Extraction

Solid phase extraction (SPE) was conducted with Strata-X cartridges (Phenomenex, Torrance, CA), which were pre-equilibrated with methanol and water. Following loading of DNA hydrolysates, cartridges were washed with 20% methanol in water. O^6-POB-G and D_4-O^6-POB-G were eluted with 100% MeOH. Samples were dried under reduced pressure, re-suspended in 15mM NH_4OAc (pH 5.5) containing 10% acetonitrile, and analyzed by the capillary HPLC-ESI$^+$-MS/MS as described below.

HPLC-ESI$^+$-MS/MS Analysis of O^6-POB-G Adducts

Capillary HPLC-ESI$^+$-MS/MS analyses were conducted using a Thermo-Finnigan Ultra TSQ mass spectrometer interfaced with a Waters Acquity capillary HPLC system. The mass spectrometer was operated in the positive ion mode. Typical spray voltage was 3.3 kV, and a capillary temperature was 250 °C. Typical tube lens offset was 91 V, and nitrogen was used as a sheath gas (43 counts). Quantitative analyses were conducted in the SRM mode, with collision energy of 13 V. Argon was used as a collision gas with a pressure of 1 mTorr. MS/MS analyses were performed with a scan width of 0.4 m/z and a scan time of 0.25 seconds.

Capillary HPLC was conducted using a Zorbax SB C18 column (0.5 mm × 150 mm, 5 μm, Agilent Technologies) eluted at a flow rate of 15 μL/min and maintained at 25°C. HPLC solvents were 15 mM ammonium acetate (A) and acetonitrile containing 15 mM ammonium acetate (10%, B). A linear gradient of 11% to 34% B in 16 minutes was used, followed by isocratic elution at 34% B for 4 minutes and column re-equilibriation.[26] Under these conditions, both O^6-POB-G and its internal standard (D_4-O^6-POB-G) eluted at ~ 14 minutes. Selected reaction monitoring (SRM) was conducted by monitoring the transitions: *m/z* 299.1 [M + H$^+$] →148.1 [POB]$^+$, *m/z* 299.1 →152.1 [Gua + H$^+$] for O^6-POB-G and *m/z* 303.1 [M + H$^+$] → m/z 152.1 ([D_4-POB]$^+$ and [Gua + H$^+$]) for D_4-O^6-POB-G.

HPLC-ESI$^+$-MS/MS method validation

Synthetic DNA 21-mers (5′-ACCCGCGTC CGCGCCATGGCC-3′, 1 pmol) were spiked with increasing amounts of the corresponding O^6-POB-dG-containing duplexes (5′-ACCCGCGTCC[O^6-POB-G]CGCCATGGCC-3′, 0.1-1pmol). DNA mixtures were dissolved in 90 μl of 50 mM Tris-HCl buffer (pH 7.8) containing 0.5 mg/mL BSA, 0.5 mM DTT, and 0.1 mM EDTA. Following the addition of D_4-O^6-POB-dG internal standard (250 fmol) and inactivated AGT protein (400 fmol), samples were subjected to mild acid hydrolysis (0.1 N HCl, 70 °C, 1h). The hydrolysates were neutralized with ammonium hydroxide and purified by solid phase extraction on Strata-X cartridges as described above. O^6-POB-G and D_4-O^6-POB-G were eluted with methanol, dried under vacuum, and re-suspended in 15 mM NH4OAc (pH 5.5) containing 10% ACN for capillary HPLC-ESI$^+$-MS/MS analyses. The validation results were expressed as the ratio of HPLC-ESI$^+$-MS/MS peak areas corresponding to O^6-POB-G and D_4-O^6-POB-G versus the actual O^6-POB-G/D_4-O^6-POB-G molar ratio. All analyses were performed in quadruplet.

Kinetics of POB Group Transfer in the Presence of Increasing Amounts of AGT

O^6-POB G-containing DNA duplexes (5′-ACCCGCGTCC[O^6-POB G]CGCCATGGCC-3′ and its compliment, 0.5 pmol, in triplicate) were dissolved in Tris-HCl buffer (50 mM, pH 7.8) containing 0.5 mg/mL BSA, 0.5 mM DTT, and 0.1 mM EDTA (final volume 90 μl). Following addition of human recombinant AGT protein (50, 200, 400, or 800 fmol), alkyl transfer reactions were allowed to proceed for varying lengths of time (0-600 seconds). Each reaction was terminated by the addition of HCl to achieve the final concentration of 0.1N. After spiking with D_4-O^6-POB-dG internal standard (250 fmol), the samples were subjected to mild acid hydrolysis(70 °C, 1h), neutralized with NH_4OH, and purified by SPE. O^6-POB-G adducts remaining in DNA after repair reaction were quantified by HPLC-ESI$^+$-MS/MS as described above.

Second Order Kinetics for AGT Reactions with O^6-POB-dG-Containing DNA

DNA duplexes containing site-specific O^6-POB-G adducts (500 fmol, Table 1) were mixed with human recombinant AGT protein (400 fmol) in 50 mM Tris-HCl buffer (pH 7.8) buffer containing 0.1 mM EDTA, 0.5 mg/mL BSA, and 0.5 mM DTT (final volume, 90 μl). Samples were incubated at room temperature for 0-50 seconds and quenched with acid (final concentration, 0.1N HCl). Following the addition of D_4-O^6-POB-dG internal standard (250 fmol), DNA was subjected to mild acid hydrolysis (1 h at 70 °C), and the unrepaired O^6-POB-dG adducts remaining in DNA were quantified by capillary HPLC-ESI$^+$-MS/MS as described above.

Second order rates (k) for AGT repair of O^6-POB-G were calculated by plotting O^6-POB-G concentrations repaired at time t (average of 4 separate measurements) versus time and fitting the data to the 2nd order kinetic equation (Equation 1) using the KaleidaGraph software:[25]

$$kt = \frac{1}{B_0 - A_0} \times \ln \frac{A_0 (B_0 - C_t)}{B_0 (A_0 - C_t)} \quad (1)$$

where A_0 is the concentration of AGT protein, B_0 is the starting concentration of O^6-POB-dG containing DNA, and C_t is the concentration of O^6-POB-G repaired at time t. The error in the reaction rate measurements was obtained from KaleidaGraph software by approximating how closely the experimentally obtained data points fit the defined 2nd order kinetic equation.

Kinetics of POB Group Transfer to the AGT Protein

DNA duplexes (5′-ACCCGCGTCC[O^6-POB-G]CGCCATGGCC-3′ (+) strand, 20 pmol) were dissolved in 50 mM Tris-HCl buffer (pH 7.8) containing 0.1 mM EDTA and 0.5 mM DTT. Following the addition of human recombinant AGT protein (16 pmol), the reaction mixtures (final volume, 90 μl) were incubated at room temperature for fixed periods of time (0 - 40 s). Each reaction was manually quenched by the addition of 0.5 N NaOH (90 μl). Samples were neutralized with HCl, dried under vacuum, and reconstituted in 100 mM ammonium bicarbonate buffer (pH 7.9, 50 μl). The protein was digested with trypsin (0.3 μg) for 18 hours at 37 °C.[27] The resulting tryptic peptides were desalted using Millipore C18 Zip Tips (Bedford, MA) and dried under reduced pressure. Samples were re-suspended in 20 μl of 0.1% formic acid and analyzed by capillary HPLC-ESI$^+$-MS/MS as described below.

Capillary HPLC-ESI$^+$-MS/MS analyses of tryptic peptides were performed with a Thermo-Finnigan Ultra TSQ mass spectrometer interfaced with a Waters Acquity capillary HPLC system. HPLC separation was achieved with a Zorbax 300 SB-C8 column (0.3 mm × 150 mm, 3.5 μm, Agilent Technologies) eluted at a flow rate of 6 μL/min and maintained at a temperature of 50 °C. HPLC solvents were aqueous 0.5% formic acid containing 0.1% trifluoroacetic acid (A) and acetonitrile containing 0.5% formic acid and 0.1% trifluoroacetic acid (B). A linear gradient of 3% to 55% B in 15 minutes was followed by isocratic elution at 55% B for 10 minutes. Under these conditions, unmodified AGT peptide eluted at ~ 24.1 minutes, while pyridyloxobutylated peptide eluted within ~ 24.5 min. The mass spectrometer was operated in the positive ion mode with a spray voltage of 3.5 kV, a capillary temperature of 250 °C, and tube lens offset of 103 V. Nitrogen was used as a sheath gas (25 counts).

Quantitative analyses were conducted in the MS/MS mode with collision energy of 24 V. Argon was used as a collision gas at a pressure of 1.3 m Torr, and all analyses were performed with a scan width of 0.3 m/z and a scan time of 0.15 s. Unmodified AGT active site peptide (G^{136}NPVPILIPCHR^{147}) was detected in the SRM mode by monitoring the transition *m/z* 658.4 $[M + 2H]^{+2} \rightarrow$ *m/z* 948.6 [y_8], while the corresponding pyridyloxobutylated peptide (G^{136}NPVPILIP[C-POB]HR^{147}) was detected using the MS/MS transition *m/z* 731.8 → *m/z* 1095.6 [y_8] (Figure 6A, Supplement S-1). The percent pyridyloxobutylation of AGT Cys-145 residue was calculated from the HPLC-ESI$^+$-MS/MS peak corresponding to the unmodified peptide containing the active site cysteine ($A_{unmodified}$) and the pyridyloxobutylated peptide (A_{POB}) according to Equation 2:

$$\%\text{pyridyloxobutylation of Cys145 of AGT} = \frac{A_{POB}}{A_{unmodified} + A_{POB}} \times 100\% \quad (2)$$

and plotted against reaction time (t) (Figure 6B).

Results

Stable Isotope labeling HPLC ESI$^+$-MS/MS Approach

As discussed above, previous methodologies have relied on radioflow HPLC or gel electrophoresis of ^{32}P endlabeled DNA oligomers to analyze the kinetics of O^6-POB-dG repair by AGT.[13,14] In the present work, a non-radioactive stable isotope labeling HPLC ESI$^+$-MS/MS approach was developed to analyze the influence of DNA sequence context on the kinetics of O^6-POB-G adduct repair by AGT. In our approach, synthetic DNA duplexes containing site specific O^6-POB-dG adducts are incubated with human recombinant AGT protein (WT h-AGT) for specified periods of time, and the reactions are quenched with HCl

(Figure 1).[19] DNA is subjected to mild acid hydrolysis to release purines, including any O^6-POB-G adducts remaining after the repair reaction, which are then quantified by isotope dilution - capillary HPLC electrospray ionization tandem mass spectrometry. Our initial studies (not shown) confirmed that no spontaneous removal of the POB group is observed under these conditions (0.1 N HCl, 70 °C, 1h). Quantitation is conducted in the selected reaction monitoring mode using the HPLC-ESI$^+$-MS/MS peak areas corresponding to O^6-POB-G and the deuterated internal standard (D_4-O^6-POB-G).

ESI$^+$-MS/MS spectrum of O^6-POB-G (*m/z* 229.0, $[M + H]^+$) is characterized by two major fragment ions at *m/z* 148.1 [POB$^+$] and *m/z* 152.1 $[Gua + H]^+$ (Figure 2A). ESI$^+$-MS/MS spectrum of D_4-O^6-POB-G (*m/z* 303.1 $[M + H]^+$) contains one main prominent peak at *m/z* 152.1, corresponding to both [D_4-POB$^+$] and $[Gua + H]^+$ (Figure 2B). Our quantitatifve method for O^6-POB-G is based on selected reaction monitoring (SRM) of the transitions *m/z* 299.1 $[M + H]^+ \rightarrow$ 148.1 [POB$^+$], *m/z* 299.1 $\rightarrow [M + H]^+ \rightarrow$ 152.1 $[Gua + H]^+$for O^6-POB-G and *m/z* 303.1 $[M + H]^+ \rightarrow$ 152.1 [D_4-POB$^+$], *m/z* 303.1 $[M + H]^+ \rightarrow$ 152.1 $[Gua + H]^+$ for D_4-O^6-POB-G internal standard (Figure 3).

HPLC separation is achieved with a capillary Zorbax SB-C18 column (Agilent Technologies) eluted at a flow rate of 15 μl/min with a gradient of 15 mM ammonium acetate and acetonitrile. Under our conditions, O^6-POB-G standard and D_4-O^6-POB-G internal standard co-elute at ~ 14 min (Figure 3). Quantitative analyses were conducted by comparing the HPLC ESI$^+$-MS/MS peak areas corresponding to O^6-POB-G and D_4-O^6-POB-G internal standard. The lower limit of detection for O^6-POB-G was estimated as 3 fmol, with a signal to noise ratio (S/N) of 3. The lower limit of quantification of O^6-POB-G adducts by our HPLC ESI$^+$-MS/MS method was estimated as 10 fmol with a signal to noise ratio of 5.

The new HPLC ESI$^+$-MS/MS method was validated by performing the analyte recovery assay. Synthetic DNA duplex (5′-ACCCGCGTCCGCGCCA TGGCC-3′ and its compliment, 1pmol) was spiked with increasing amounts of the corresponding O^6-POB-dG-containing duplex (5′-ACCCGCGTCC[O^6-POB-G]CGCCA TGGCC-3′ and its compliment, 0.1-1pmol) and acid-inactivated recombinant AGT protein (WT h-AGT, 400 fmol). The resulting mixtures were subjected to mild acid hydrolysis, followed by sample processing and capillary HPLC-ESI$^+$-MS/MS analysis as described above. The observed O^6-POB-G/ D_4-O^6-POB-G ratios were plotted against the theoretical ratios of O^6-POB-G/ D_4-O^6-POB-G (Figure 4). A linear correlation with an R^2 value of 0.9965 and a slope of 1.0254 was obtained, validating our quantitative HPLC-ESI$^+$-MS/MS method for O^6-POB-G adducts in DNA.

Time Course of AGT Repair within p53 codon 158 Derived DNA Sequences

To test the applicability of our analytical methodology to studies of AGT repair kinetics, time dependent repair of O^6-POB-dG in the presence of increasing amounts of human recombinant AGT protein was investigated. Synthetic oligodeoxynucleotide duplexes representing codon 158 of the *p53* tumor suppressor gene and surrounding sequence were prepared containing O^6-POB-dG adduct at the second position of *p53* codon 158 (5′-ACCCGCGTCC[O^6-POB-G]CGCCATGGCC-3′, (+) strand). Following annealing to the complementary strand, the resulting site-specifically modified duplexes were incubated with 0.1-1.6 equivalents of human recombinant AGT protein over fixed periods of time (0-600 s), and O^6-POB-dG adducts remaining in DNA were quantified by HPLC ESI$^+$-MS/MS.

The repair ratios for the control samples (R_0) consisted of peak area of O^6-POB-G/ D_4-O^6-POB-G in DNA alone (time t = 0 sec), while repair ratios at time = t (R_t) was obtained by analyzing ratios of area of O^6-POB-G/ D_4-O^6-POB-G upon incubation of DNA with AGT

protein for a given time (Equation 3). The percent repair (% repair) of O^6-POB-dG was obtained by calculating the difference in repair of control samples and repaired DNA at a given time followed by dividing this value by the repair ratio of the control sample times 100% (Equation 3).[25]

$$\%\text{Repair}=\frac{R_0 - R_t}{R_0} \times 100\% \quad (3)$$

A plot of % repair versus time revealed a time- and concentration-dependent removal of O^6-POB-dG adducts by AGT (Figure 5). As expected for second order kinetics, increased AGT concentrations resulted in a proportional increase in the rate of O^6-POB-G repair. The extent of DNA dealkylation increased proportionately until ~ 60 s, after which no additional repair was observed for the remainder of the incubation due to the depletion of active AGT protein as a result of alkyl group transfer to Cys-145 (Scheme 1). We have previously observed similar results for AGT-mediated repair of O^6-methyl-dG adducts.[19]

Mass Spectrometry-based Detection of Pyridyloxobutylated AGT Protein

As discussed above, AGT repair reaction involves alkyl group transfer from DNA to an active site cysteine of the protein (Cys-145 in human AGT).[7] To investigate the kinetics of protein pyridyloxobutylation in the presence of O^6-POB-dG-containing DNA, AGT repair reactions with *p53* codon 158 containing DNA duplexes (5′-ACCCGCGTCC[O^6-POB-G]CGCCATGGCC-3′+ complement) were quenched with NaOH, and the time-dependent formation of alkylated protein was followed by capillary HPLC-ESI-MS/MS analysis of the tryptic peptide G^{136}NPVPILIPC^{145}HR^{147} corresponding to AGT active site containing cysteine 145 (Cys-145). Both intact (M = 1314.4 Da) and pyridyloxobutylated AGT active site peptide (M = 1461.6 Da, POB group = 147 Da) were detected using selected reaction monitoring of the y_8 fragment formation from doubly charged pseudo-molecular ions of the peptides of interest (*m/z* 658.2→ 948.6 for unmodified peptide and *m/z* 731.8 →1095.6 for pyridyloxobutylated peptide; see Figure 6A). HPLC-ESI-MS/MS peak areas corresponding to the intact and alkylated peptide were compared to calculate the extent of protein pyridyloxobutylation. A time-dependent increase in the concentration of pyridyloxobutylated protein was observed until ~ 15 seconds, after which the concentrations of pyridyloxobutylated protein formed leveled off due to the depletion of active protein (Figure 6B). The reaction rate was faster than that in the experiments shown in Figure 5 due to the increased concentrations of DNA substrate and AGT protein used in this experiment. Higher protein amounts were required to facilitate the detection of pyridyloxobutylated active site peptide.

Kinetics of AGT Repair of O^6-POB-G Adducts within DNA Sequence Representing codon 12 of the rat H-ras Gene

The new HPLC-ESI-MS/MS methodology was employed to analyze the kinetics of AGT-mediated POB transfer from O^6-POB-dG-containing DNA duplexes derived from rat *H-ras* gene as a function of the partner base in the opposite strand. Synthetic DNA duplexes (5′-AATAGTATCT[O^6-POB-G]GAGCC-3′, where O^6-POB-G is placed at the first position of *H-ras* codon 12 were prepared containing either C or T opposite O^6-POB-G. Following incubation of adducted duplexes with recombinant human AGT protein for defined periods of time, the reactions were quenched with acid, spiked with D_4-O^6-POB-dG internal standard, and the amounts of O^6-POB-G adducts remaining in DNA were determined by isotope dilution capillary HPLC ESI^+-MS/MS. This was used to calculate the amounts of O^6-POB-G adducts removed at time t (Figure 7). A graph of O^6-POB-G concentrations repaired versus time was obtained, and the resulting curves were fitted to the 2nd order

kinetics equation (Equation 4) using KaleidaGraph software (Synergy Software, Reading, PA)[25,28]:

$$kt = \frac{1}{B_0 - A_0} \times \ln \frac{A_0 (B_0 - C_t)}{B_0 (A_0 - C_t)} \quad (4)$$

where A_0 is the molar concentration of AGT protein, B_0 is the molar concentration of *O*^{6}-POB-G containing DNA duplex, C_t is the concentration of *O*^{6}-POB-G adducts repaired at time t, t is the time in seconds, and k is the 2nd order rate for *O*^{6}-POB-G repair.

Kinetic analysis have yielded the 2nd order rates of 1.17 ± 0.05 × 10^6 $M^{-1}s^{-1}$ for repair of *O*^{6}-POB-G paired with C and 1.74 ± 0.1 × 10^6 $M^{-1}S^{-1}$ for *O*^{6}-POB-G mispaired with T (Figure 7).

Discussion

The presence of functional AGT protein is crucial for cellular protection against alkylating agents such as nitrosamines present in tobacco smoke.[3,4] If not repaired, *O*^{6}-alkylguanines can pair with a T or A instead of C during DNA replication, leading to G → A transitions and G → T transversion mutations.[5] Human cancers with reduced expression levels of the AGT protein have an increased frequency of G → A mutations in the *K-ras* protooncogene and the *p53* tumor suppressor gene as compared to tumors with normal expression of AGT,[29-32] indicative of a major protective function of AGT protein against these genetic changes. Epigenetic silencing of the *MGMT* gene coding for AGT has been correlated with susceptibility for tumor development following exposure to alkylating agents.[33]

Previous studies have revealed that the efficiency of AGT-mediated repair of *O*^{6}-alkylguanines is affected by adduct structure, local sequence context, and the identity of the base in the opposite strand.[34] The relative rates of AGT-mediated repair of *O*^{6}-alkyl-dG lesions have been reported as benzyl > methyl > ethyl >> 2-hydroxyethyl >4-(3-pyridyl)-4-oxobutyl, probably due to a slower rate of transfer of bulky alkyl groups to the active site cysteine when they are bound in an inactive conformation.[14,34]

AGT repair involves several distinct kinetic steps that have different rates.[28] Following binding to the minor groove of DNA, AGT protein flips the adducted nucleotide out of the DNA base stack to enter the protein active site pocket, while Arg128 takes the place of the adducted nucleotide in the DNA duplex.[6,9] The alkyl group is then transferred from the *O*^{6}-position of guanine to the active site cysteine of AGT *via* an in-line displacement reaction, and finally, the alkylated AGT dissociates from the repaired DNA. The rate of AGT binding to DNA appears to be diffusion-limited (5 × 10^9 M^{-1} s^{-1}) and is unaffected by the identity of the alkyl group on the *O*^{6}-alkyl-dG lesion or the nucleotide sequence surrounding the lesion,[14] while the rate of protein dissociation is slower.[28] The rate of AGT-mediated nucleotide flipping is between 80 and 200 s^{-1} [25] and is equally efficient for methyl and benzyl adducts.[28] The alkyl transfer step appears to be rate limiting for *O*^{6}-Me-dG and *O*^{6}-POB-dG adducts, although the rates of alkyl transfer have not been measured directly, but calculated from the rates for all of the other steps in the reaction.[28]

In our earlier work, we have developed a quantitative HPLC ESI^+-MS/MS methodology for analyzing the kinetics of AGT-mediated repair of *O*^{6}-methyl-dG adducts *in vitro*.[19,25] Our analyses have employed second-order kinetics, as explained by a simple bimolecular reaction between the AGT protein and its DNA substrate (Scheme 1). Under these conditions, AGT repair of *O*^{6}-methyl-dG exhibited a moderate sequence dependence, with

~2-fold differences between the rate of repair of O^6-Me-dG located at the first and the second position of human *K-ras* codon 12.[19] The dealkylation rate was weakly influenced by the methylation status of neighboring cytosine bases due to its effects on the rate of alkyl transfer.[25] While the overall effects of sequence context on O^6-Me-dG repair by AGT were modest, due to the stochiometric nature of AGT reaction, even small differences in substrate preference may influence the probability of lesion repair at specific sites within the genome.[8]

In comparison to O^6-Me-dG, AGT-mediated repair of bulky alkylguanine adducts such as O^6-[4-oxo-4-(3-pyridyl)but-1-yl]deoxyguanosine (O^6-POB-dG) appears to be more strongly affected by the local DNA sequence context.[13,14] As discussed above, O^6-POB-dG is an important DNA lesion induced by tobacco-specific nitrosamines NNK and NNN and playing an important role in the carcinogenic mechanism of NNK.[4,5] In general, AGT repair of O^6-POB-dG is less efficient than that of O^6-Me-dG, probably due to the larger adduct size and the possibility of adduct binding to AGT active site in a non-reactive conformation.[14] Coulter et al. and Mijal et al. previously reported that the first order rate for AGT repair of O^6-POB-dG placed at the first guanine of *H-ras* codon 12 was greater as compared to adducts present at the second G.[13,14] However, to our knowledge, there has been no systematic study of the effects of DNA sequence on AGT-mediated repair of O^6-POB-dG lesions.

In the present work, a non-radioactive, sensitive, and accurate isotope dilution HPLC-ESI$^+$-MS/MS methodology was developed to analyze the kinetics of O^6-POB-dG adduct repair by AGT. In our approach, DNA duplexes containing site-specific DNA adducts are incubated with recombinant human AGT protein for fixed periods of time, followed by acid hydrolysis and HPLC-ESI$^+$-MS/MS analysis of O^6-POB-G adducts remaining in DNA over time. Since no separation of alkylated and dealkylated strands is required, this methodology is highly reliable and is applicable to AGT repair studies with DNA of any sequence and length.

The applicability of the new method was demonstrated by analyzing the kinetics of AGT-mediated repair of O^6-POB-dG lesions placed within the context of *p53* codon 158 in the presence of increasing AGT amounts (Figure 5). As expected, the rate of O^6-POB-dG repair increased proportionally as the AGT amounts were raised. Saturation of repair was observed when using low AGT:DNA ratios due to the depletion of active protein. As was the case with O^6-Me-dG,[19] we did not observe quantitative repair of O^6-POB-dG lesions even when using 1.6 molar excess protein under these *in vitro* conditions, which could be a result of cooperative AGT-DNA binding[10] and/or the competition of active protein with alkylated protein for binding to the DNA substrate.[8]

Second order rates of AGT-mediated repair of O^6-POB-dG placed at the first position of rat *H-ras* codon 12 were determined with cytosine or thymine opposite the adduct. We found that the rate of AGT repair was 1.5 fold faster for the O^6-POB-dG:T base pair than for the O^6-POB-dG:C pair ($1.74 \pm 0.1 \times 10^6$ $M^{-1}s^{-1}$ versus $1.17 \pm 0.05 \times 10^6$ $M^{-1}s^{-1}$) (Figure 7). This observation is consistent with an earlier report by Mijal et al.,[13] who demonstrated that placing a thymine opposite a O^6-POB-dG adduct caused an increase in AGT mediated repair as compared to O^6-POB-dG:C base pair. By comparison, the rates of AGT-mediated repair of O^6-Me-dG:C placed in a similar sequence context (*K-ras* codon 12) are 5-10 times greater ($7.4\text{ -}14 \times 10^6$ $M^{-1}s^{-1}$).[19,34] Our ongoing investigations (not shown) suggest that this difference in repair rates is due to a combination of slower nucleotide flipping and alkyl transfer steps in the case of bulky O^6-POB-dG adducts.

In conclusion, an accurate and general isotope dilution capillary HPLC ESI$^+$-MS/MS method has been developed to investigate the rates of AGT mediated repair of O^6-POB-dG

adducts as a function of local DNA sequence. This methodology will be useful for future investigations of the kinetics of AGT-mediated repair of pyridyloxobutylated DNA adducts.

Supplementary Material

Refer to Web version on PubMed Central for supplementary material.

Acknowledgments

We thank Dr. Stephen S. Hecht (University of Minnesota Cancer Center) for D_4-O^6-POB-dG internal standard and Dr. Lisa Peterson (University of Minnesota Cancer Center) for O^6-POB-dG-containing oligomer derived from the rat *H-ras* gene. We are grateful to Brock Matter and Dr. Peter Villalta (Analytical Biochemistry and Mass Spectrometry Facility at the Cancer Center, University of Minnesota) for their assistance with mass spectrometry analyses and Robert Carlson (University of Minnesota Masonic Cancer Center) for preparing figures for this manuscript.

Funding Support This work was funded by a grant from the National Cancer Institute (CA-095039).

Reference List

1. Hecht SS, Chen CB, Ohmori T, Hoffmann D. Comparative carcinogenicity in F344 rats of the tobacco-specific nitrosamines, N'-nitrosonornicotine and 4-(N-methyl-N-nitrosamino)-1-(3-pyridyl)-1-butanone. Cancer Res. 1980; 40:298–302. [PubMed: 7356512]
2. Hecht SS, Morse MA, Amin S, Stoner GD, Jordan KG, Choi CI, Chung FL. Rapid single-dose model for lung tumor induction in A/J mice by 4-(methylnitrosamino)-1-(3-pyridyl)-1-butanone and the effect of diet. Carcinogenesis. 1989; 10:1901–1904. [PubMed: 2791206]
3. Hecht SS. Biochemistry, biology, and carcinogenicity of tobacco-specific N-nitrosamines. Chem. Res. Toxicol. 1998; 11:559–603. [PubMed: 9625726]
4. Hecht SS. DNA adduct formation from tobacco-specific N-nitrosamines. Mutat. Res. 1999; 424:127–142. [PubMed: 10064856]
5. Pauly GT, Peterson LA, Moschel RC. Mutagenesis by O^6-[4-oxo-4-(3-pyridyl)butyl]guanine in *Escherichia coli* and human cells. Chem. Res. Toxicol. 2002; 15:165–169. [PubMed: 11849042]
6. Daniels DS, Woo TT, Luu KX, Noll DM, Clarke ND, Pegg AE, Tainer JA. DNA binding and nucleotide flipping by the human DNA repair protein AGT. Nat. Struct. Mol. Biol. 2004; 11:714–720. [PubMed: 15221026]
7. Pegg AE. Repair of O^6-alkylguanine by alkyltransferases. Mutat. Res. 2000; 462:83–100. [PubMed: 10767620]
8. Pegg AE. Multifaceted roles of alkyltransferase and related proteins in DNA repair, DNA damage, resistance to chemotherapy, and research tools. Chem. Res. Toxicol. 2011; 24:618–639. [PubMed: 21466232]
9. Tubbs JL, Pegg AE, Tainer JA. DNA binding, nucleotide flipping, and the helix-turn-helix motif in base repair by O^6-alkylguanine-DNA alkyltransferase and its implications for cancer chemotherapy. DNA Repair. 2007; 6:1100–1115. [PubMed: 17485252]
10. Fried MG, Kanugula S, Bromberg JL, Pegg AE. DNA Binding mechanism of O^6-alkylguanine-DNA alkyltransferase: Stoichiometry and effects of DNA base composition and secondary structure on complex stability. Biochemistry. 1996; 35:15295–15301. [PubMed: 8952480]
11. Major GN, Brady M, Notarianni GB, Collier JD, Douglas MS. Evidence for ubiquitin-mediated degradation of the DNA repair enzyme for O^6-methylguanine in non-tumour derived human cell and tissue extracts. Biochem. Soc. Trans. 1997; 25:359S. [PubMed: 9191404]
12. Gouws C, Pretorius PJ. O(6)-methylguanine-DNA methyltransferase (MGMT): Can function explain a suicidal mechanism? Med. Hypotheses. 2011
13. Mijal RS, Kanugula S, Vu CC, Fang Q, Pegg AE, Peterson LA. DNA Sequence context affects repair of the tobacco-specific adduct O^6-[4-oxo-4-(3-pyridyl)butyl]guanine by human O^6-alkylguanine-DNA alkyltransferases. Cancer Res. 2006; 66:4968–4974. [PubMed: 16651455]

14. Coulter R, Blandino M, Tomlinson JM, Pauly GT, Krajewska M, Moschel RC, Peterson LA, Pegg AE, Spratt TE. Differences in the rate of repair of O^6-alkylguanines in different sequence contexts by O^6-alkylguanine-DNA alkyltransferase. Chem. Res. Toxicol. 2007; 20:1966–1971. [PubMed: 17975884]
15. Wang L, Spratt TE, Liu XK, Hecht SS, Pegg AE, Peterson LA. Pyridyloxobutyl adduct O^6-[4-oxo-4-(3-pyridyl)butyl]guanine is present in 4-(acetoxymethylnitrosamino)-1-(3-pyridyl)-1-butanone-treated DNA and is a substrate for O^6-alkylguanine-DNA alkyltransferase. Chem. Res. Toxicol. 1997; 10:562–567. [PubMed: 9168254]
16. Gait, MJ. Oligonucleotide synthesis: a practical approach. IRL Press; Washington, DC: 1984.
17. Edara S, Kanugula S, Goodtzova K, Pegg AE. Resistance of the human O^6-alkylguanine-DNA alkyltransferase containing arginine at codon 160 to inactivation by O^6-benzylguanine. Cancer Res. 1996; 56:5571–5575. [PubMed: 8971155]
18. Liu L, Xu-Welliver M, Kanugula S, Pegg AE. Inactivation and degradation of O^6-alkylguanine-DNA alkyltransferase after reaction with nitric oxide. Cancer Res. 2002; 62:3037–3043. [PubMed: 12036910]
19. Guza R, Rajesh M, Fang Q, Pegg AE, Tretyakova N. Kinetics of O^6-Me-dG repair by O^6-alkylguanine DNA alkyltransferase within *K-ras* gene derived DNA sequences. Chem. Res. Toxicol. 2006; 19:531–538. [PubMed: 16608164]
20. Wang L, Spratt TE, Pegg AE, Peterson LA. Synthesis of DNA oligonucleotides containing site-specifically incorporated O^6-[4-oxo-4-(3-pyridyl)butyl]guanine and their reaction with O^6-alkylguanine-DNA alkyltransferase. Chem. Res. Toxicol. 1999; 12:127–131. [PubMed: 10027788]
21. Matter B, Wang G, Jones R, Tretyakova N. Formation of diastereomeric benzo[*a*]pyrene diol epoxide-guanine adducts in *p53* gene-derived DNA sequences. Chem. Res. Toxicol. 2004; 17:731–741. [PubMed: 15206894]
22. Ziegel R, Shallop A, Upadhyaya P, Jones R, Tretyakova N. Endogenous 5-methylcytosine protects neighboring guanines from N7 and O^6-methylation and O^6-pyridyloxobutylation by the tobacco carcinogen 4-(methylnitrosamino)-1-(3-pyridyl)-1-butanone. Biochemistry. 2004; 43:540–549. [PubMed: 14717610]
23. Tretyakova N, Matter B, Jones R, Shallop A. Formation of benzo[*a*]pyrene diol epoxide-DNA adducts at specific guanines within *K-ras* and *p53* gene sequences: stable isotope-labeling mass spectrometry approach. Biochemistry. 2002; 41:9535–9544. [PubMed: 12135376]
24. Ziegel R, Shallop A, Jones R, Tretyakova N. *K-ras* gene sequence effects on the formation of 4-(methylnitrosamino)-1-(3-pyridyl)-1-butanone (NNK)-DNA adducts. Chem. Res. Toxicol. 2003; 16:541–550. [PubMed: 12703972]
25. Guza R, Ma L, Fang Q, Pegg AE, Tretyakova N. Cytosine methylation effects on the repair of O^6-methylguanines within CG dinucleotides. J. Biol. Chem. 2009; 284:22601–22610. [PubMed: 19531487]
26. Rajesh M, Wang G, Jones R, Tretyakova N. Stable isotope labeling-mass spectrometry analysis of methyl- and pyridyloxobutyl-guanine adducts of 4-(methylnitrosamino)-1-(3-pyridyl)-1-butanone in *p53*-derived DNA sequences. Biochemistry. 2005; 44:2197–2207. [PubMed: 15697245]
27. Loeber R, Rajesh M, Fang Q, Pegg AE, Tretyakova N. Cross-linking of the human DNA repair protein O^6-alkylguanine DNA alkyltransferase to DNA in the presence of 1,2,3,4-diepoxybutane. Chem. Res. Toxicol. 2006; 19:645–654. [PubMed: 16696566]
28. Zang H, Fang Q, Pegg AE, Guengerich FP. Kinetic analysis of steps in the repair of damaged DNA by human O^6-alkylguanine-DNA alkyltransferase. J. Biol. Chem. 2005; 280:30873–30881. [PubMed: 16000301]
29. Wolf P, Hu YC, Doffek K, Sidransky D, Ahrendt SA. O^6-Methylguanine-DNA methyltransferase promoter hypermethylation shifts the *p53* mutational spectrum in non-small cell lung cancer. Cancer Res. 2001; 61:8113–8117. [PubMed: 11719438]
30. Esteller M, Toyota M, Sanchez-Cespedes M, Capella G, Peinado MA, Watkins DN, Issa JP, Sidransky D, Baylin SB, Herman JG. Inactivation of the DNA repair gene O^6-methylguanine-DNA methyltransferase by promoter hypermethylation is associated with G to A mutations in *K-ras* in colorectal tumorigenesis. Cancer Res. 2000; 60:2368–2371. [PubMed: 10811111]

31. Bello MJ, Alonso ME, Aminoso C, Anselmo NP, Arjona D, Gonzalez-Gomez P, Lopez-Marin I, de Campos JM, Gutierrez M, Isla A, Kusak ME, Lassaletta L, Sarasa JL, Vaquero J, Casartelli C, Rey JA. Hypermethylation of the DNA repair gene MGMT: association with TP53 G:C to A:T transitions in a series of 469 nervous system tumors. Mutation Research/Fundamental and Molecular Mechanisms of Mutagenesis. 2004; 554:23–32.

32. Nakamura M, Watanabe T, Yonekawa Y, Kleihues P, Ohgaki H. Promoter methylation of the DNA repair gene MGMT in astrocytomas is frequently associated with G:C −> A:T mutations of the TP53 tumor suppressor gene. Carcinogenesis. 2001; 22:1715–1719. [PubMed: 11577014]

33. Wirtz S, Nagel G, Eshkind L, Neurath MF, Samson LD, Kaina B. Both base excision repair and O^6-methylguanine-DNA methyltransferase protect against methylation-induced colon carcinogenesis. Carcinogenesis. 2010; 31:2111–2117. [PubMed: 20732909]

34. Guza R, Pegg AE, Tretyakova N. Effects of sequence context on O^6-alkyltransferase repair of O^6-alkyldeoxyguanosine adducts. ACS Symposium Series. 2010; 1041:73–101.

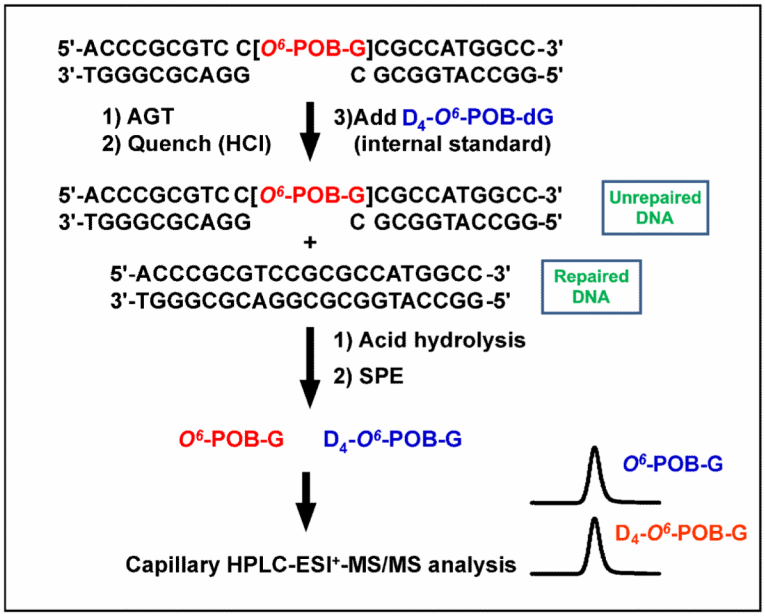

Figure 1.
HPLC-ESI$^+$-MS/MS methodology employed for quantitative analyses of O^6-POB-G adducts remaining in DNA following AGT repair.

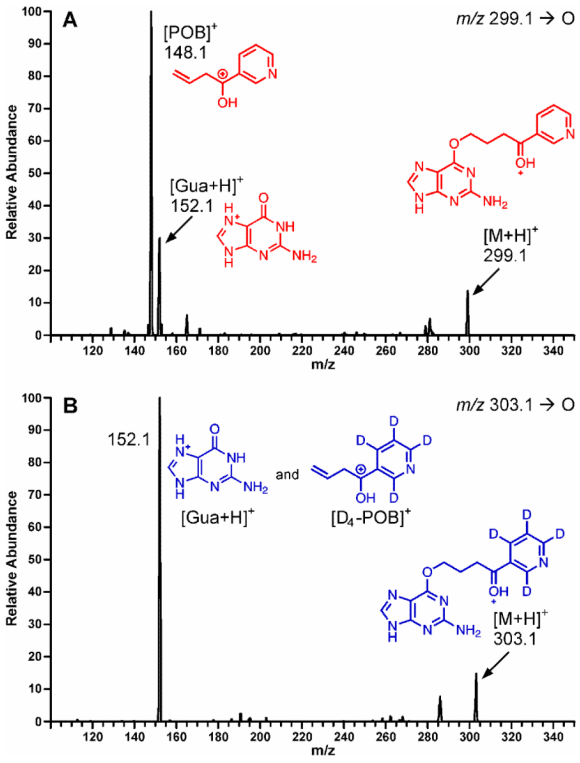

Figure 2.

ESI$^+$-MS/MS spectra of O^6-POB-G (A) and D_4-O^6-POB-G (B) and proposed structures of the major fragments.

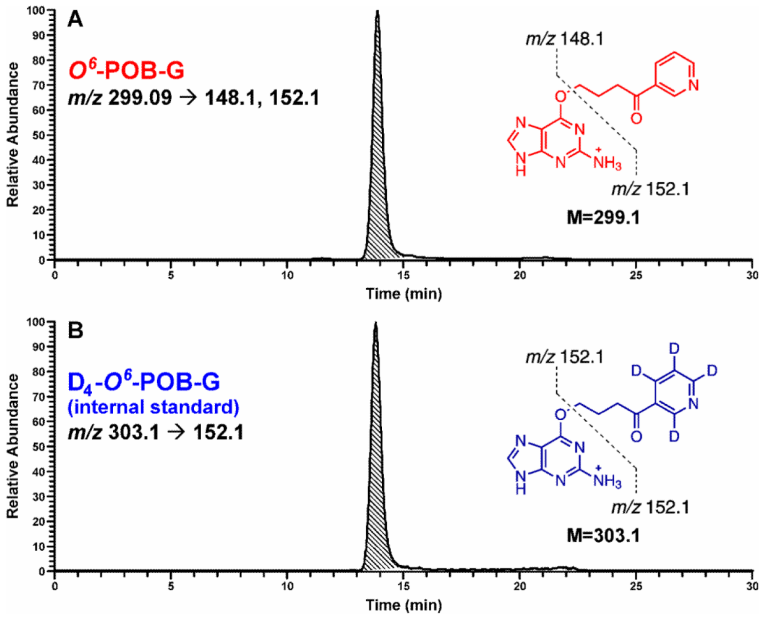

Figure 3.

Capillary HPLC-ESI$^+$-MS/MS analysis of O^6-POB-G adducts remaining in DNA following AGT repair reaction. 500 fmol of double-stranded DNA (5′-ACCCGCGTCC[O^6-POB-G]CGCCATGGCC-3′ and its compliment) was incubated with 400 fmol of AGT protein for 20 seconds, followed by quenching with HCl and spiking with 250 fmol of D_4-O^6-POB-dG. The resulting mixture was subjected to acid hydrolysis and analyzed by capillary HPLC-ESI$^+$-MS/MS. The mass spectrometer was operated in SRM mode by monitoring the transitions *m/z* 299.09 [M + H$^+$] →148.1 [POB$^+$], 152.07 [Gua + H$^+$] for O^6-POB-G (A) and *m/z* 303.09 [M + H$^+$]→152.07[D_4-POB$^+$], [Gua + H$^+$] for D_4-O^6-POB-G (B).

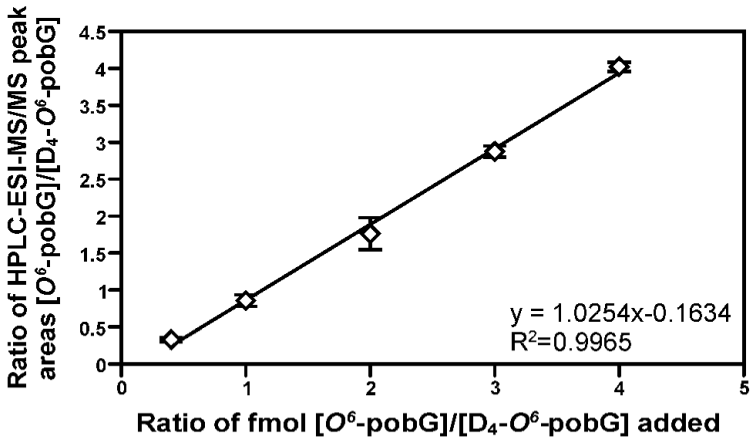

Figure 4.

Validation results for quantitative capillary HPLC-ESI$^+$-MS/MS method for O^6-pobG using isotope dilution with D$_4$-O^6-POB-G internal standard. Synthetic O^6-pob-dG-containing DNA duplex (5′-ACCCGCGTCC[O^6-POB-G]CGCCATGGCC-3′ and its compliment, 0.1-1pmol) was mixed with the corresponding native DNA duplex (1 pmol), D$_4$-O^6-POB-dG internal standard, and acid-inactivated AGT protein (500 fmol)(N=4). The resulting mixtures were subjected to mild acid hydrolysis, and O^6-POB-G adducts were quantified by capillary HPLC-ESI$^+$-MS/MS. The results are expressed as a ratio of HPLC-ESI-MS/MS peak areas corresponding to O^6-POB-G and D$_4$-O^6-POB-G versus the actual O^6-POB-G|D$_4$-O^6-POB-G molar ratio.

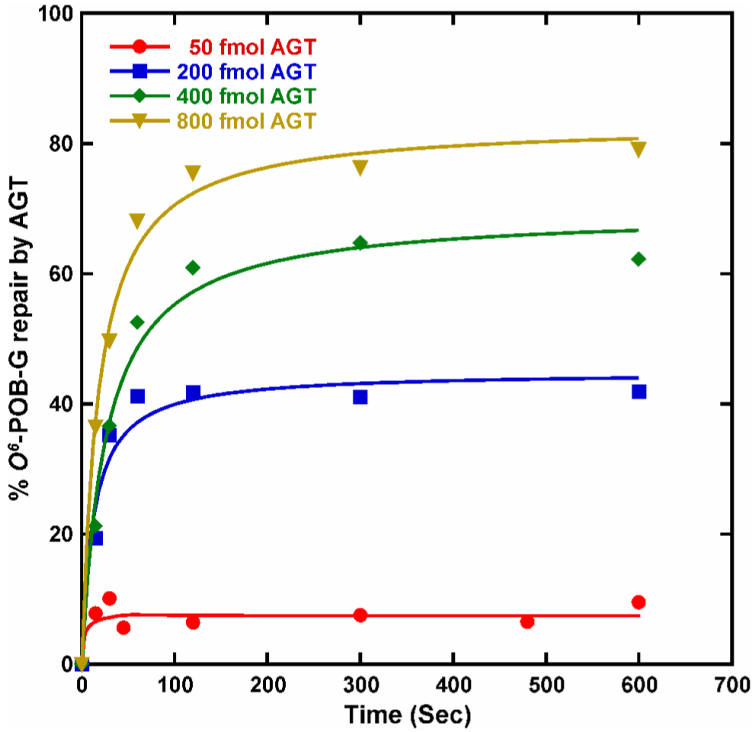

Figure 5.

Time course for the repair of O^6-POB-G adducts incorporated into synthetic DNA duplexes (5′-ACCCGCGTCC[O^6-POB-G]CGCCATGGCC-3′ and its compliment) in the presence of increasing amounts of recombinant human AGT protein (20, 200, 400, or 800 fmol). O^6-POB-G adducts remaining in DNA following the specified reaction times were quantified by isotope dilution HPLC-ESI$^+$-MS/MS. The line was generated by fitting to a single-exponential equation using KaleidaGraph software.

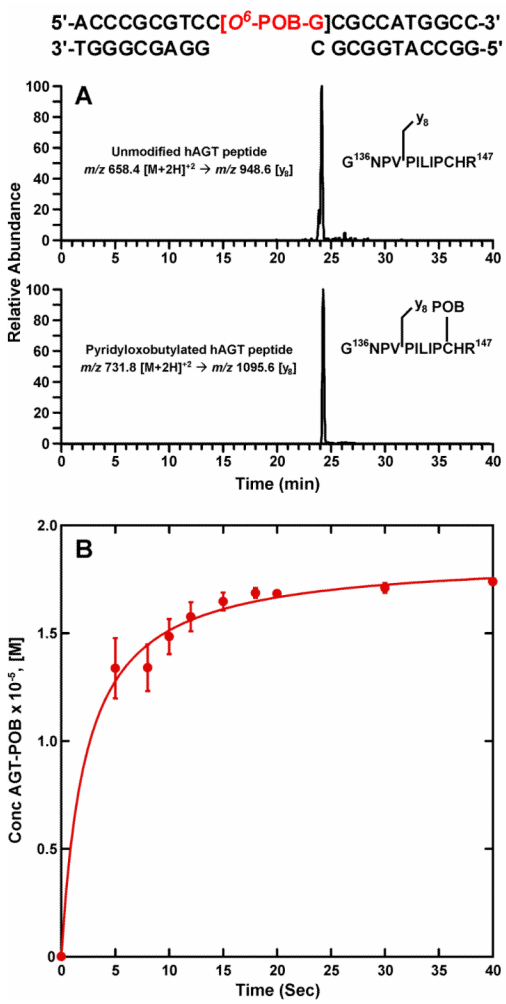

Figure 6.

Formation of pyridyloxobutylated AGT protein following incubation with O^6-POB-dG-containing DNA duplex (5′-ACCCGCGTCC[O^6-POB-G]CGCCATGGCC-3′ and its compliment): Capillary HPLC-ESI$^+$-MS/MS analysis of pyridyloxobutylated AGT active site peptide (G^{136}NPVPILIPCHR) (A). Time course for the formation of pyridyloxobutylated AGT protein (B). The line was generated by fitting the data to a single exponential equation using KaleidaGraph software.

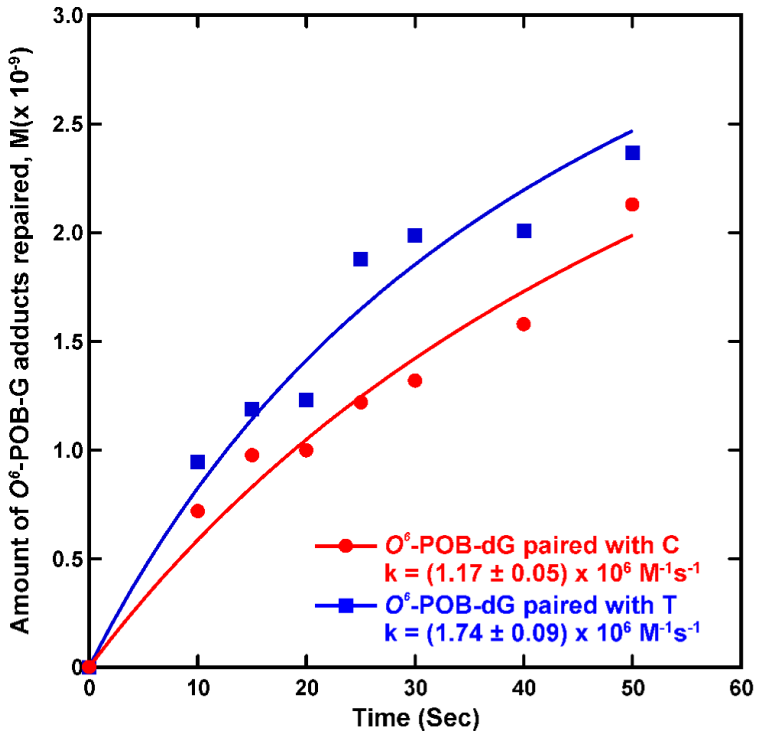

Figure 7.

AGT repair kinetics for O^6-POB-dG adducts placed opposite dC or dT in synthetic DNA duplexes (5′-AATAGTATCT[O^6-POB-G]GAGCC-3′ + strand) containing either C or T opposite the adducts). DNA (500 fmol) was incubated with human recombinant AGT protein (400 fmol) for increasing lengths of time (0-50 seconds). The reactions were stopped by HCl quenching, and unrepaired O^6-POB-G adducts were quantified by isotope dilution HPLC-ESI$^+$-MS/MS. Each data point represents an average of four independent measurements. The curves represent the best fit to a second-order exponential equation that provides the rate of O^6-POB-dG repair by AGT obtained by the KaleidaGraph software. The error is estimated by determining how closely the second order kinetic equation fits the actual data points.

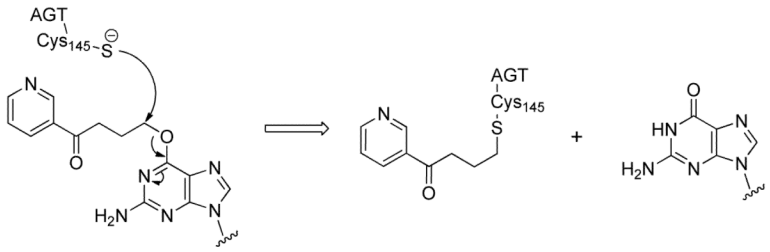

Scheme 1.
AGT repair of O^6-pyridyloxobutyl-dG adducts in DNA

Table 1

Nucleobase sequence and molecular weight information (from HPLC2ESI^{2}2MS) for synthetic DNA oligomers employed in this work.

Oligomer	Sequence	Molecular Weight	
		Calculated	Observed
(+) p53 codon 158-O^6pobG	ACCCGCGTCC[O^6-POB-G]CGCCATGGCC	6026.0	6026.9
(−) p53 codon 158	GGCCATGGC GCG GACGCGGGT	6529.3	6529.4
(+) p53 codon 158	ACCCGCGTCCGCGCCATGGCC	6329.1	6328.8
(+) *H-ras* POB	AATAGTATCT[O^6-POB-G]GAGCC	5052.3	5051.7
(−) *H-ras* base paired dC	GGCTCCAGATACTATT	4856.2	4855.6
(−) *H-ras* base paired dT	GGCTCTAGATACTATT	4871.2	4870.7